

## Supplemental information for “Selective GaSb Radial Growth on Crystal Phase Engineered InAs Nanowires”

Luna Namazi<sup>1</sup>, Malin Nilsson<sup>1</sup>, Sebastian Lehmann<sup>1</sup>, Claes Thelander<sup>1</sup>, Kimberly A. Dick<sup>1,2</sup>

<sup>1</sup> *Solid State Physics, Lund University, Box 118, S-221 00 Lund, Sweden*

<sup>2</sup> *Center for Analysis and Synthesis, Lund University, Box 124, S-221 00 Lund, Sweden*

### Table of Contents

<i>S1. Optimization of InAs core crystal structure for different diameters</i> .....	2
S2. Time dependence of GaSb shell growth .....	4
S3. Time dependence of GaSb shell growth .....	5
S4. Seed particle density effect .....	7
S5. Material composition of the axial GaSb segment .....	8
S6. Elemental maps of Sb and In on the multiple segmented nanowires .....	9

## ***S1. Optimization of InAs core crystal structure for different diameters***

For different seed particle diameters specific growth timings with different flows and pressures of the precursors were used in order to obtain the optimized InAs core structure. After loading the InAs samples inside the reactor, the temperature was raised to 550 °C for 7 minutes to anneal the sample and remove any oxide on the surface of the substrate. An AsH<sub>3</sub> flow ranging from  $7.69 \times 10^{-5}$  to  $1.54 \times 10^{-2}$  was present in the reactor, starting from the annealing step, until the InAs core growth was completed in order to avoid InAs from decomposing at high temperatures. After the annealing step the temperature was ramped down to 460 °C. For Au particles with 40 nm diameter, the InAs nanowire growth was commenced by providing a TMIn flow equal to ( $3.48 \times 10^{-6}$ ) while the AsH<sub>3</sub> flow was switched to ( $1.92 \times 10^{-2}$ ) to nucleate the growth from the seed particle. The first wurtzite segment (WZ1) was then grown for 5 minutes at a lower AsH<sub>3</sub> flow of  $9.23 \times 10^{-5}$ , while keeping the TMIn flow constant. For growing the zinc blende segment a significantly higher V/III ratio is required. Therefore, a higher AsH<sub>3</sub> flow ( $1.54 \times 10^{-2}$ ) was provided into the reactor for a set time depending on the desired length of the zinc blende segment (5 minutes in figure S1). Then after, the AsH<sub>3</sub> flow was switched to the set values for wurtzite growth ( $9.23 \times 10^{-5}$ ) and the second wurtzite segment was grown for 2 minutes.

Since tuning the crystal phase becomes more sensitive to growth conditions as the diameter of the Au seed particle gets smaller, in order to optimize the crystal structure for Au particles with 30nm diameters, different TMIn flows for the different structures were used in contrary to the constant TMIn flow utilized for both WZ and ZB segments for diameter of 40nm. Also, pausing steps were introduced in between consecutive segments of the InAs core structure. This was done to allow time to purge away excess material from the reactor, while switching the AsH<sub>3</sub> flows. During these short pausing steps TMIn was switched off, and the samples remained under an AsH<sub>3</sub> flow. The TMIn flow used for the wurtzite segments was slightly higher ( $3.48 \times 10^{-6}$ ) compared to that used for growing the zinc blende segment ( $1.93 \times 10^{-6}$ ). The pausing time used between wurtzite and zinc blende was 45s, whereas it was set to 3s when switching from zinc blende to wurtzite. For attaining a better understanding, figure S1 depicts the sequence of flows and pausing steps of the growth of an InAs core with a WZ-ZB-WZ structure. Growth times for the different segments for 30 nm samples that were similar to those of 40 nm, lead to longer segments as expected e.g. for 5 minutes of ZB growth 450 nm versus 300 nm, and for 5 minutes of WZ2 growth time 550 nm versus 400 nm for nanowires with particle diameters of 30 nm and 40 nm respectively. The lengths of different segments were tailored to desire by adjusting the growth times based on the diameter and areal particle density.

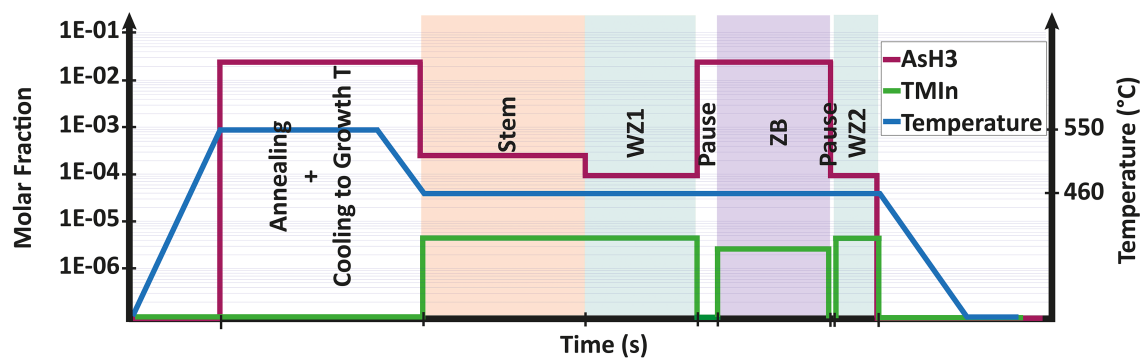


Figure S1: Schematics for set temperatures, precursor flows, and precursor switching as used for growing an InAs core structure from Au seed particles of 30nm versus time. The molar fraction is demonstrated with a logarithmic scale on the left y-axis, while the right y-axis shows the temperature. The time axis is to scale with the real values used for growing the nanowires.

## S2. Time dependence of GaSb shell growth

Starting from the reference shell growth time (20 minutes), 3 additional growth times, 10, 40, and 60 minutes were investigated. From the 30° tilted SEM images (S2a-d) and the analysis given in S2e it can be seen that neither the shell thickness around the ZB segment, nor the diameter of the axial GaSb do not considerably change as time increases (S2e). The offset from the trend of the data point related to 40 minutes can be explained by the Au aerosol nanoparticle variability and the diameter spread caused by this artefact. On the other hand, the axial growth rate increases with time (S2f). Therefore, it can be concluded that at these growth conditions, longer shell growth times do not necessarily lead to thicker shells on the ZB segments since the material is all consumed by the axial growth of the axial GaSb segment.

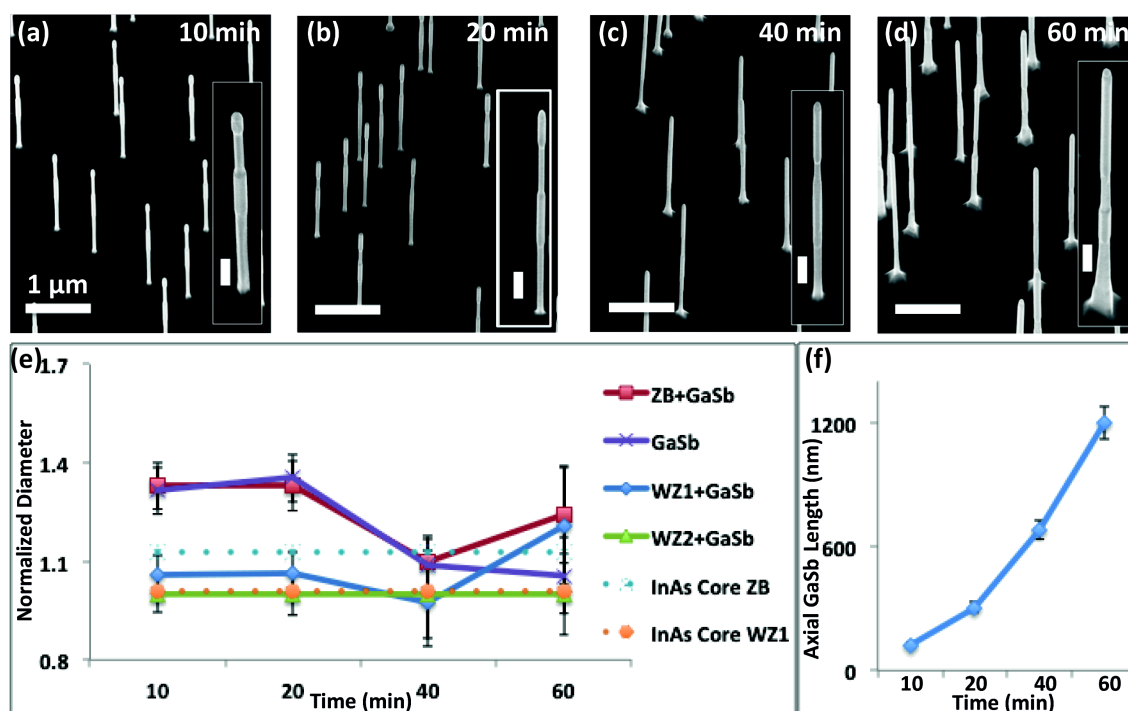


Figure S2: 30°-tilted SEM images of the GaSb shell growth time series of a) 10, b) 20, c) 40, and d) 60 minutes. The scale bar corresponds to 1 μm. Insets in a-d show a higher magnification image of a representative nanowire highlighting the different axial segments. The measured diameter of the various nanowire segments is given in (e), normalized to the WZ core diameter, and for the different shell growth times. Please note that for WZ1 the error bars on 40 and 60 minutes of shell growth time are relatively large, showing a large variation in nanowire diameter caused by the spread in the aerosol particle diameter or due to unstable growth conditions. Taking this into consideration, the diameter of the WZ1 segment can be considered constant; independent from the GaSb shell growth time.

### **S3. Total precursor flow influence on GaSb shell growth**

A series of different total precursor flows was also carried out under a constant nominal V/III ratio of 1.6. Starting from the reference recipe's total precursor flow of  $8.87 \times 10^{-5}$  (the sum of the molar fractions of the group III and V precursors), two additional flows were studied, namely  $4.44 \times 10^{-5}$  and  $17.0 \times 10^{-5}$ . As seen in image S3, at the lower total flow the GaSb shell on the zinc blende segment is asymmetric, growing on only one of the side facets of the ZB. The SEM image in figure S3a and b indicates that the nanowires are bent probably due to the strain between the InAs core and the GaSb shell caused by the asymmetric shell growth. From this figure it is also observable that the distribution of this one facet-growth selectivity is statistically equal for all three facets. Therefore the measurements done on the diameter of the zinc blende are not reliable as they do not represent a value corresponding to a uniform shell layer thickness around the zinc blende. One can relate this to a kinetic process when nucleation is initiated on one facet leading to the preference of growth continuation on that facet only. We speculate that this is due to a very low nucleation rate of the GaSb layer. Once nucleation occurs on one side facet, continuation of growth on that side facet is more favoured than nucleation on other facets, leading to the formation of these asymmetrical shells.

Other than that, the two experiments with higher total flows (figures S3c, and d) show uniform shell (thickness) formation. It is clear from the graph in figure S3e that the diameter of the axial GaSb segment and the zinc blende diameter have opposite trends, meeting in the mid point. In other words, relating this to the increment observed in figure S3f in the length of the axial GaSb segment, it can be stated that as the amount of precursors in the reactor increases the axial GaSb segment growth becomes dominant related to the competition between the radial shell growth on the zinc blende segment and the axial GaSb growth. At the medium total precursor flow the radial growth rates of both the ZB segment and the axial GaSb are more or less equal to each other.

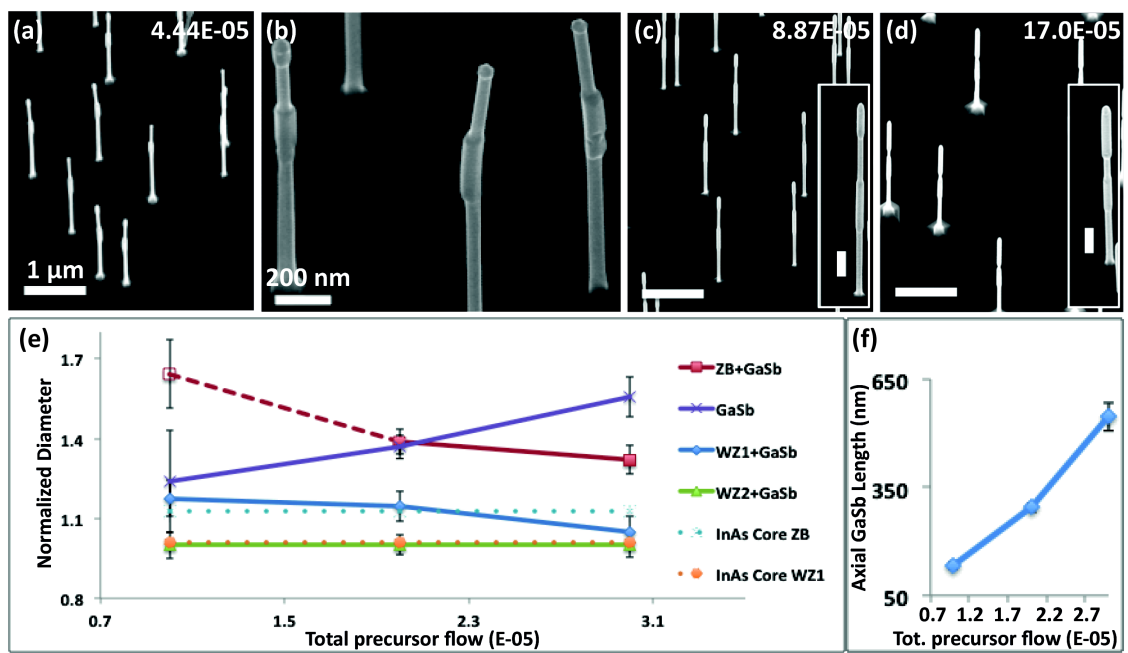


Figure S3: Total flows of a)  $4.44 \times 10^{-5}$ , c)  $8.87 \times 10^{-5}$ , and d)  $17.0 \times 10^{-5}$  of the GaSb shell precursors. In a) asymmetric shells are observed on the zinc blende segments of the nanowires. The three-fold asymmetrical shell formation is clearly observable from the zoomed in image displayed in (b). d) The normalized diameter of the different segments of the core-shell nanowires for different shell growth times. e) demonstrates a linear increment in the length of the axial GaSb segment for increasing total flows which is explained by the presence for more material in the reactor during growth.

#### S4. Seed particle density effect

The areal density of the deposited Au seed particles has a big influence on the length and morphology of the grown nanowires.

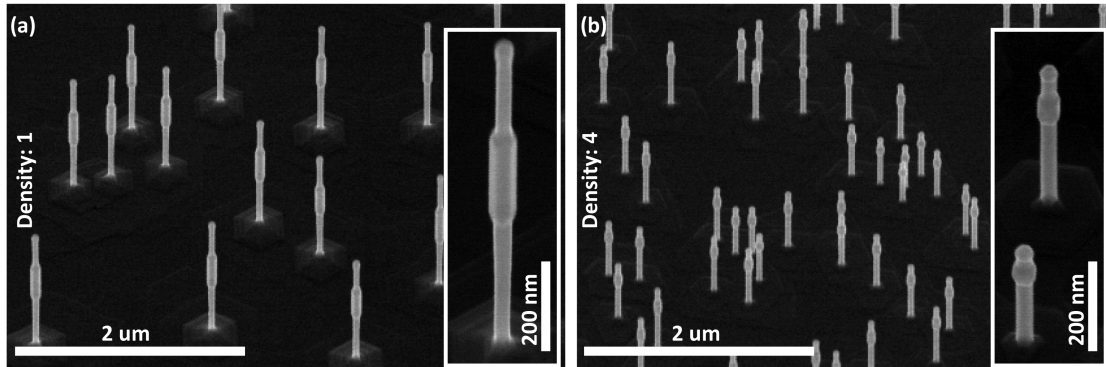


Figure S4: SEM images of core/shell InAs GaSb nanowires grown from Au seed particles with a diameter of 40 nm and an areal density of (a) 1 particle/ $\mu\text{m}^2$ , and (b) 4 particle/ $\mu\text{m}^2$  grown under the exact same conditions. Due to competition for material the nanowires with a higher surface density have a lower growth rate, leading to shorter length of the different segments. Also, at higher densities a nanowire to nanowire variation is observed, which is again related to material competition at the growth sites.

## S5. Material composition of the axial GaSb segment

Under certain shell growth conditions an axial GaSb segment grows above the WZ2 segment. In figure S5 the XEDS map analysis confirms that this segment is pure GaSb and is not an InAs segment related to the core structure.

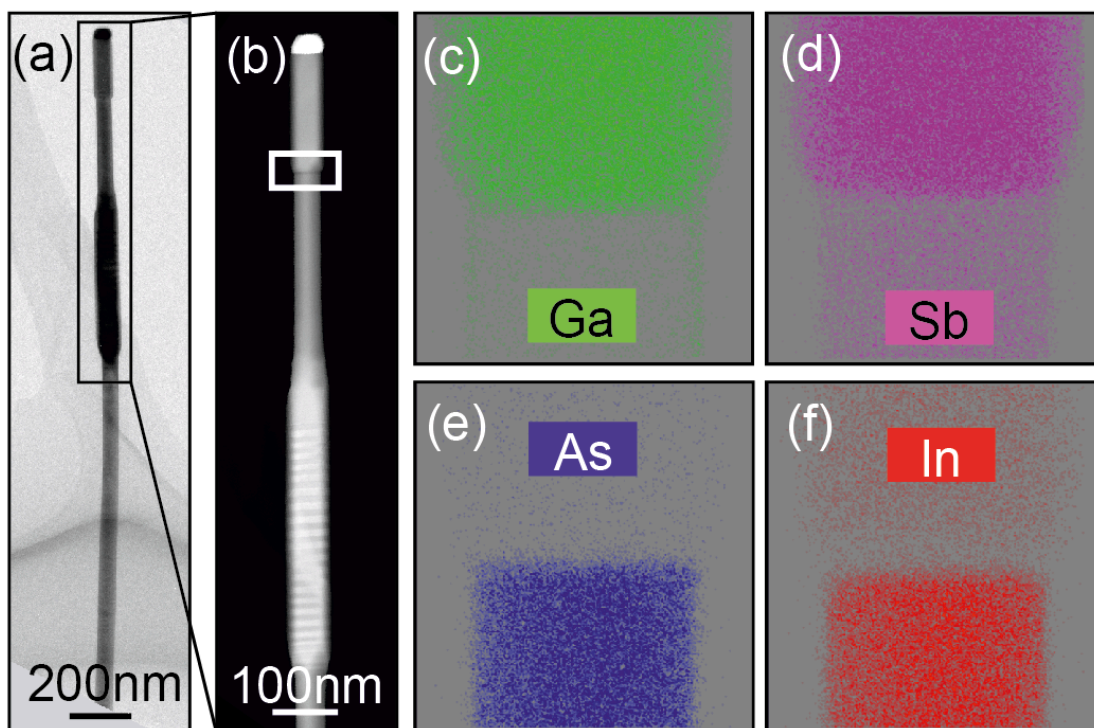


Figure S5: a) TEM overview of a core-shell InAs-GaSb nanowire where the black box indicates where the higher magnification dark field image in (b) is corresponding to. The transition between the WZ2 segment and the top axial GaSb segment is represented by the white box in (b). c-f) XEDS elemental maps acquired from the area indicated by the white box in b). These maps confirm that the top segment is pure GaSb with no traces of the core InAs.

## S6. Elemental maps of Sb and In on the multiple segmented nanowires

A full elemental map of all the elements of the core and shell are given here. However, it is worth noting that due to the overlap between the Sb  $L_{\alpha}$  line and the In  $L_{\beta}$  line, distinguishing In and Sb, is not as straight forward. Therefore, it ruling out the In trace from the shell and the Sb trace from the core is not completely feasible. In addition, the GaSb shell entirely surrounds the InAs core on the ZB segments. This leads to uncertainty in determining the existence of interdiffusion based on the XEDS technique.

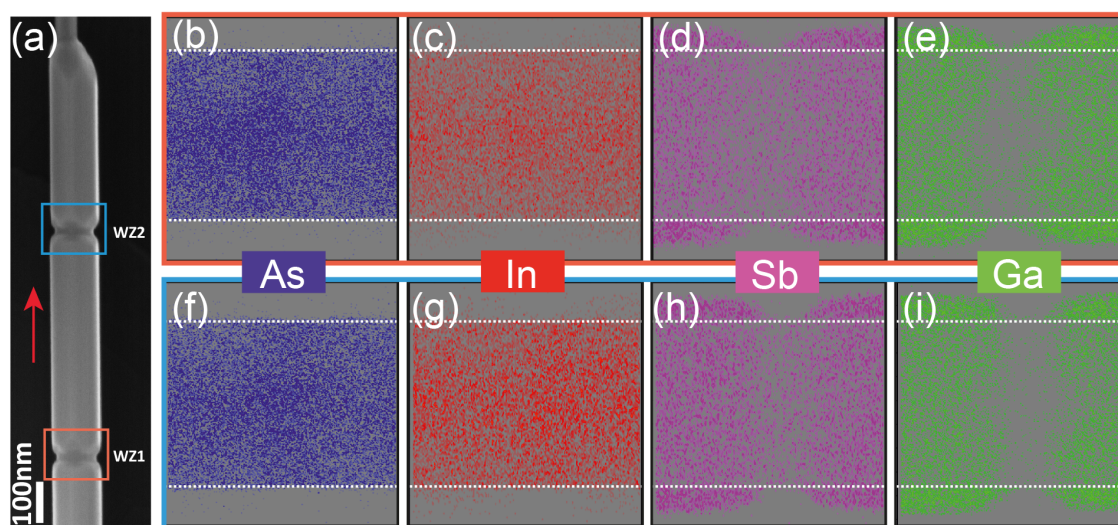


Figure S6: a) SEM image of a multiple segmented InAs/GaSb core/ shell nanowire. The red arrow shows the growth direction. The colored boxes correspond to the XEDS maps of all the composing material of both the core (In and As) and the shell (Ga and Sb) shown in figures S6 b-i.